Two-dimensional dam-break simulation over movable beds with an unstructured mesh

José A. Vásquez
Northwest Hydraulic Consultants, North Vancouver, Canada

João G.A.B. Leal
University of Beira Interior, Covilha, Portugal

ABSTRACT: This paper reports the application of a two-dimensional (2D) depth-averaged model to dam break flows over alluvial sand beds with an initial bed step. The model applies the Finite Element Method to discretize the computational domain using an unstructured mesh made of triangular elements. Two downstream boundary conditions were tested: zero (dry) and non-zero (wet) initial water depths. The model successfully reproduced the two types of transient waves observed in the experiments: the hydraulic jump produced with wet downstream condition and the surge moving over an initially dry bed. Since the present sediment transport model applied a single layer for sediment transport, comparison and discussion with results of a previous one-dimensional (1D) two-layer model are also provided.

1 INTRODUCTION

1.1 *Dam-breaks and movable beds*

Dam-break flows can lead to highly unsteady flows with fast-moving wave fronts. Traditionally, dam-break phenomenon has been studied under fixed-bed conditions. However, movable beds can affect the celerity of flood waves propagating in rivers after a dam-break. Even more, the wave celerity is influenced by the sediment mobility (Capart & Young 1998, Leal et al. 2002, Fraccarollo & Capart 2002, Cao et al. 2004, Leal et al. 2006). Therefore, dam-break analysis on rivers requires the inclusion of the effects of alluvial bed on the flow hydraulics.

Dams represent an obstacle to the normal sediment transport in a river, inducing sediment deposition upstream from the dam, as well as bed erosion downstream. For an existing dam in an alluvial river, a bed elevation difference will develop between the riverbed elevations upstream and downstream from the dam. During a real dam-break event, it is very likely that a movable bed step will exist at the location of the dam that will impact how the flood wave propagates downstream.

Leal et al. (2002) conducted experimental dam-break research that incorporated the effects of both sediment mobility and bed steps on wave propagation. These experiments provide high-quality data under more realistic conditions than simpler experiments conducted on flat fixed-beds. Leal et al. (2003a,b) successfully simulated these experimental observations using a one-dimensional (1D) numerical model.

In this paper, the two-dimensional (2D) numerical model developed by Vasquez (2005a) is applied to simulate two of the experimental tests of Leal et al. (2002) of dam-breaks over sand beds with an initial bed step. One distinctive feature of the model is the application of an unstructured (irregular) mesh made of triangular Finite Elements. The main objective of the present work is to verify the applicability of such model to dam-break flows over movable beds. Additionally, some qualitative tests of bed changes in a varying width flume, and a dam-break in a sharp 90^o bend over a fixed bed, are presented to show the 2D capabilities of the model.

1.2 *Background information*

Vasquez (2005a) developed a 2D river morphology model by extending the existing fixed-bed hydrodynamic model River2D (Steffler & Blackburn 2002). This new movable-bed version is referred as River2D-MORphology. River2D-MOR has been successfully applied to reproduce experiments of bed aggradation and degradation in straight flumes (Vasquez et al. 2005a, Vasquez et al. 2006a), scour and deposition in laboratory bends (Vasquez et al. 2005b) and meandering rivers (Vasquez et al. 2006b), as well as knickpoint migration under transcritical flow conditions (Vasquez et al. 2005c). Preliminary qualitative tests (Vasquez 2005a) suggested that River2D-MOR could be applied to dyke-breach and dam-break analysis. However, until now, it has not been tested quantitatively to verify if the model

is indeed suitable for dam-breaks over movable beds.

The main features of River2D-MOR at the moment are (Vasquez 2005a):

– unstructured Finite Element (FE) mesh;
– simulates bedload sediment transport;
– free or forced upstream sediment inflow;
– transcritical flow capabilities;
– secondary flow correction for flow in bends;
– incorporates the effects of transverse bed slope on bedload direction.

Unstructured meshes have the advantage of being more flexible that structured (regular) meshes. Triangular elements allow to easily accommodate practically any planform river geometry with elements that can dramatically change in size to obtained higher resolution around areas of interest. For example, structured meshes based on quadrilateral elements can be problematic in certain channel geometries with sharp angles (Heer & Mosselman 2004), for which triangular elements are perfectly suitable (Vasquez 2005b). River2D-MOR is a decoupled model, that is, sediment equations are solved after the flow equations.

The remaining of the paper is organized as follows. In section 2, information of the hydrodynamic model is briefly introduced; later a qualitative application to dam-break in a channel with a sharp bend is shown to demonstrate the 2D capabilities of the model. In section 3, the bedload model is introduced along with an example application to an alluvial channel with a continuously changing width. In section 4, a description of the experimental tests of dam-break over movable beds is provided. The results of the model are presented in section 5. The discussion of the paper are presented in Section 6. Finally, summary and conclusions are presented in Section 7.

2 HYDRODYNAMIC MODEL

2.1 *River2D*

River2D is a fixed-bed hydrodynamic model that has been developed at the University of Alberta in Canada (it is freely available at www.River2D.ca). River2D is based on the 2D depth-averaged Saint-Venant equations expressed in conservative form; which form a system of three equations representing the conservation of water mass and the two components of the momentum vector. The model is intended for use on natural streams and rivers and has special features for supercritical/subcritical flow transitions, ice covers, and variable wetted area. River2D handles dry beds by changing the surface flow equations to groundwater flow equations in areas where the water depth drops below a minimum value. A continuous free surface with positive (above ground) and negative (below ground) depths is calculated. This procedure allows calculations to carry on without changing or updating the boundary conditions (Steffler and Blackburn 2002).

For the spatial discretization River2D uses a flexible FE unstructured mesh composed of triangular elements. The Finite Element Method used by River2D is based on the Streamline Upwind Petrov-Galerkin (SUPG) weighted residual formulation (numerical details of the model are shown in Ghanem et al. 1995). In this technique, upstream biased test functions are used to ensure solution stability under the full range of flow conditions, including subcritical, supercritical, and transcritical flow. A fully conservative discretization is implemented which ensures that no fluid mass is lost or gained over the modeled domain. This also allows implementation of boundary conditions as natural flow or forced conditions.

The equations solved by the River2D are (Steffler and Blackburn 2002):
The water continuity equation:

$$\frac{\partial h}{\partial t}+\frac{\partial q_x}{\partial x}+\frac{\partial q_y}{\partial y}=0 \tag{1}$$

The vertically averaged momentum equation in the x-direction:

$$\frac{\partial q_x}{\partial t}+\frac{\partial (uq_x)}{\partial x}+\frac{\partial (vq_x)}{\partial y}+\frac{g}{2}\frac{\partial h^2}{\partial x}=$$

$$gh\left(S_{ox}-S_{fx}\right)+\frac{1}{\rho}\left(\frac{\partial (h\tau_{xx})}{\partial x}+\frac{\partial (h\tau_{xy})}{\partial y}\right) \tag{2}$$

The vertically averaged momentum equation in the y-direction:

$$\frac{\partial q_y}{\partial t}+\frac{\partial (uq_y)}{\partial x}+\frac{\partial (vq_y)}{\partial y}+\frac{g}{2}\frac{\partial h^2}{\partial y}=$$

$$gh\left(S_{oy}-S_{fy}\right)+\frac{1}{\rho}\left(\frac{\partial (h\tau_{yx})}{\partial x}+\frac{\partial (h\tau_{yy})}{\partial y}\right) \tag{3}$$

where t = time, h = water depth; (u,v) = depth-averaged velocities in the (x,y) directions; $q_x = uh$ = flow discharge in x-direction per unit width; $q_y = vh$ = flow discharge in the y-direction per unit width; (S_{ox},S_{oy}) = bed slopes in the (x,y) directions; S_{fx} and S_{fy} = corresponding friction slopes; τ_{xx}, τ_{xy}, τ_{yx}, τ_{yy} = components of the horizontal turbulent stress tensor; ρ = water density; and g = gravitation acceleration.

The basic assumptions in equations (1) through (3) are (Steffler and Blackburn 2002):

– The pressure distribution is hydrostatic, which limits the accuracy in areas of steep slopes and rapid changes in bed slopes.

– The horizontal velocities are constant over the depth. Information on secondary flows and circulations is not available.
– Coriolis and wind forces are assumed negligible.

The friction slope terms depend on the bed shear stresses which are assumed to depend on the magnitude and direction of the vertically averaged velocities. For example, in the *x* direction:

$$S_{fx} = \frac{\tau_{bx}}{\rho g h} = \frac{\sqrt{u^2 + v^2}}{g h C_*^2} u \tag{4}$$

τ_{bx} is the bed shear stress in the *x* direction and C_* is the dimensionless Chezy coefficient, which is related to the effective roughness height k_s through

$$C_* = 5.75 \log\left(12 \frac{h}{k_s}\right) \quad ; \quad \frac{h}{k_s} \geq \frac{e^2}{12} \tag{5a}$$

$$C_* = 2.5 + \frac{30}{e^2}\left(\frac{h}{k_s}\right) \quad ; \quad \frac{h}{k_s} < \frac{e^2}{12} \tag{5b}$$

e = 2.7182; C_* is related to Chezy's C coefficient through

$$C_* = \frac{C}{\sqrt{g}} \tag{6}$$

The depth-averaged turbulent shear stresses are modeled with a Boussinesq type eddy viscosity. For example:

$$\tau_{xy} = \upsilon_t \left(\frac{\partial u}{\partial y} + \frac{\partial v}{\partial x}\right) \tag{7}$$

where υ_t = eddy viscosity coefficient, which is assumed as composed of three components: a constant, a bed shear generated term, and a transverse shear generated term

$$\upsilon_t = \varepsilon_1 + \varepsilon_2 \frac{h\sqrt{u^2 + v^2}}{C_*} + \ldots$$

$$\varepsilon_3^2 h^2 \sqrt{2\frac{\partial u}{\partial x} + \left(\frac{\partial u}{\partial y} + \frac{\partial v}{\partial x}\right)^2 + 2\frac{\partial v}{\partial y}} \tag{8}$$

The default value for ε_1 is 0. This coefficient can used to stabilize the solution for very shallow flows when the second term in equation (8) may not to adequately describe υ_t for the flow. Reasonable values for ε_1 can be calculated by evaluating the second term in equation (8) using average flow conditions (average flow depth and average velocities) for the modeled site. The default value for ε_2 is 0.5. By analogy with transverse dispersion coefficients in rivers, values of 0.2 to 1.0 are reasonable. Since most river turbulence is generated by bed shear, this term is usually the most important. In deeper lake flows, or flows with high transverse velocity outlets gradients, transverse shear may be the dominant turbulence generation mechanism. Strong recirculation regions are important examples. In these cases, the third term, ε_3, becomes important. It is essentially a 2D (horizontal) mixing length model. The mixing length is assumed to be proportional to the depth of flow. A typical value for ε_1 is 0.1, but this may be adjusted by calibration.

In the present application, assuming that turbulence is bed-generated, the default values of the model ε_1= 0, ε_2= 0.5 and ε_3= 0 were adopted. A qualitative application to a dam-break test case is shown below for illustration purposes.

2.2 *Dam-break in channel with 90^o bend*

Soares Frazão et al. (2001) and Soares Frazão & Zech. (2002) performed experiments of dam-break through a sharp 90^o bend, which consisted of a 2.44 m by 2.39 m upstream reservoir connected to a 0.495 m wide rectangular channel. The upstream channel reach is about 4 m long while the downstream reach, after the bend, is about 3 m long. The downstream end of the channel is open. The sudden raise of the gate between the upstream reservoir and the channel is used to simulate the dam break.

After dam-break, water flows rapidly into the channel and reflects against the bend wall, where a bore forms that travels back in the upstream direction towards the reservoir. Using a 2D Finite Volume model, Aureli et al. (2004) have recently simulated one of the experiments with an initial water level in the reservoir of 0.20 m above the initially dry channel bed. To simulate the free fall at the downstream end an artificial high slope slide was introduced in the numerical model. The same experiment was used for the present qualitative application.

In River2D a constant roughness k_s = 5 mm was set throughout the model. Although it is possible to use a downstream boundary condition similar to that used by Aureli et al. (2004), given the illustrative purposes of this test a simple downstream boundary condition with zero depth was assumed. Therefore, the results presented are only qualitative.

Figure 1 shows snapshots of the computed water surface at different times. At t = 7 s the reflection in the bend wall becomes evident. Figure 2 shows the comparison between the computed profile and the levels recorded at 6 gauges. Gauge G1 is located at the center of the reservoir, while gauges G2 through G6 at located along the centerline of the channel.

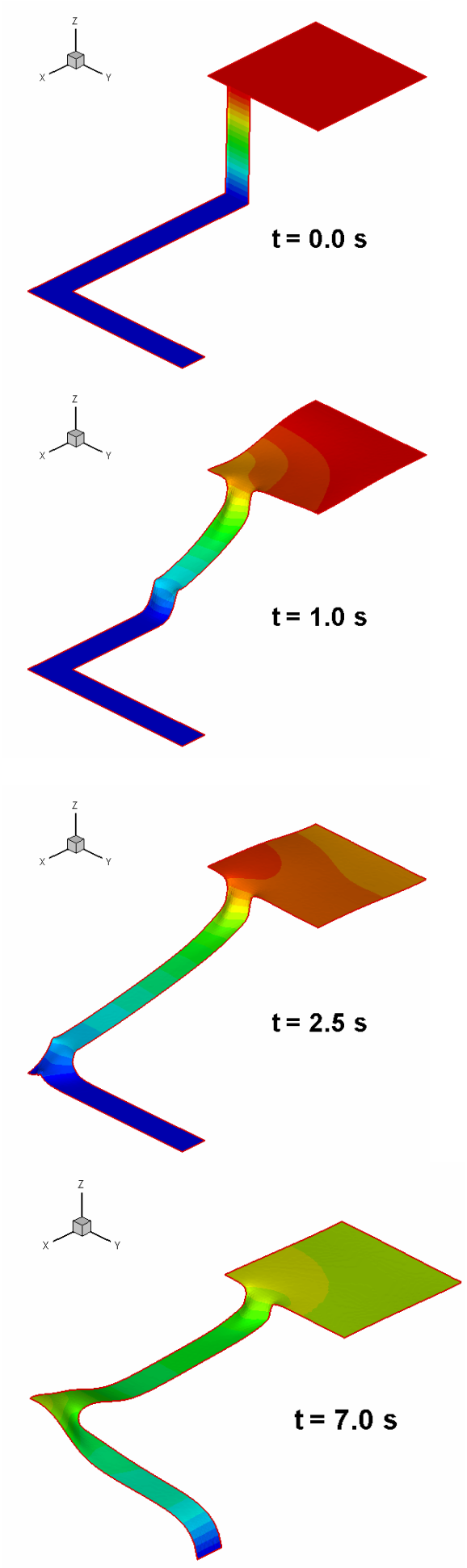

Figure 1. Computed water surfaces for a dam-break in a channel with a 90° sharp bend.

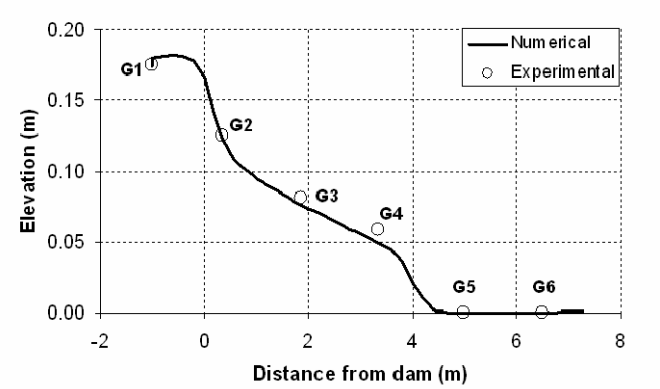

Figure 2. Experimental and numerical results at 2.5 s for dam break through a 90° bend.

Figure 2 shows that the model produces reasonable results at the beginning of the simulation when the effects of the downstream end are still not important. However, the accuracy of the results deteriorates as time progresses because of the constant downstream water level enforced by the model.

3 BEDLOAD MODEL

River2D was extended by Vasquez (2005a) to incorporate a solver for the bed load sediment continuity (Exner) equation

$$(1-\lambda)\frac{\partial z_b}{\partial t}+\frac{\partial q_{sx}}{\partial x}+\frac{\partial q_{sy}}{\partial y}=0 \qquad (9)$$

where z_b = bed elevation; λ = porosity of the bed material (with a default value of 0.4); and (q_{sx}, q_{sy}) = components of the volumetric rate of bedload transport per unit width q_s that depend on the direction α of sediment transport:

$$q_{sx} = q_s \cos\alpha \qquad (10a)$$

$$q_{sx} = q_s \sin\alpha \qquad (10b)$$

In a straight flume, where the direction of bedload and mean flow coincide, the direction of bedload in equation (10) is simply tan α = (v/u). However, in curved channels the secondary flow produces a deviation between the depth-averaged flow direction and the direction δ of the bed shear stress

$$\delta = \arctan\left(\frac{v}{u}\right) - \arctan\left(A\frac{h}{r_c}\right) \qquad (11)$$

The term -arctan(Ah/r_c) is the deviation of the bed shear stress relative to the streamlines, caused by the secondary flow. A is a parameter of order 10 and r_c is the curvature of the streamlines computed from the flow field as

$$r_c = \frac{(u^2 + v^2)^{3/2}}{-uv\frac{\partial u}{\partial x} - v^2\frac{\partial u}{\partial y} + u^2\frac{\partial v}{\partial x} + uv\frac{\partial v}{\partial y}} \quad (12)$$

The direction of bedload is computed taking into account the effects of the bed slopes $\partial z_b/\partial x$ and $\partial z_b/\partial y$ along the x and y coordinates respectively

$$\tan\alpha = \frac{\sin\delta - \frac{1}{f_s\tau^*}\frac{\partial z_b}{\partial y}}{\cos\delta - \frac{1}{f_s\tau^*}\frac{\partial z_b}{\partial x}} \quad (13)$$

τ^* is the dimensionless shear stress or Shield's parameter and f_s is a shape factor of order 1. The applicability of the secondary flow model (equations 11 through 13) has been demonstrated for both curved flumes (Vasquez et al. 2005b) and meandering rivers (Vasquez et al. 2006b).

Equation (9) is discretized using a conventional Galerkin Finite Element Method (GFEM). The time advance is performed using a Runge-Kutta second order scheme. Since GFEM lacks upwinding properties (equivalent to a central difference scheme) it is known to be adequate for diffusive problems, but not for advection-dominated problems (Donea & Huerta 2003, Vasquez 2005a). The model should not be applied to problems where advection is important, such as migrating bedforms or sediment waves. An illustrative application showing the formation of forced bars in a sand-bed channel is presented below.

3.1 *Application to varying width flume*

Tsujimoto (1987) reported experiments of bed level changes in an initially flat alluvial channel with continuous expansions and contractions, produced by changing the channel width $B(x)$ according to a sinusoidal function

$$B(x) = B_o - B_1 \sin(2\pi x / L) \quad (14)$$

The only experimental data provided by Tsujimoto (1987) are related to channel plan geometry: B_o = 0.19 m, B_1 = 0.04 m and L = 0.40 m. No more details of the experiment are given such as sediment size, inflow, downstream water level, bed slope, roughness or sediment transport rate, preventing a quantitative comparison with any particular experiment. The measured bed profiles showed very rich bed variability. The transverse concavity of the bed profiles switches from downward across the narrowest section to upward across the widest section. Across the narrow section a central bar develops, while across the wide section two lateral bars are present near the walls. In contrast with free alternate bars in straight channels, which migrate in the downstream direction, the bars formed in the channel with varying width remain fixed in position, similar to the point bars formed in alluvial bends.

For the numerical simulation, the following values were adopted: discharge 0.0056 m^3/s, depth 0.07 m, bed slope 0.001, roughness k_s = 0.0014 m, A = 2 and f_s = 2. The computational mesh was made of nodes spaced roughly 1 cm apart. Sediment transport was computed using the Engelund-Hansen equation for a 1 mm sand grain. Figure 3 shows the plan view of the computed results after 1000 s using a time step of 1 s. The model correctly predicts the concavity of the bed and the formation of bars. Figure 4 shows the pattern of lateral and central bars computed by the model which agrees, at least qualitatively, with the experimental results.

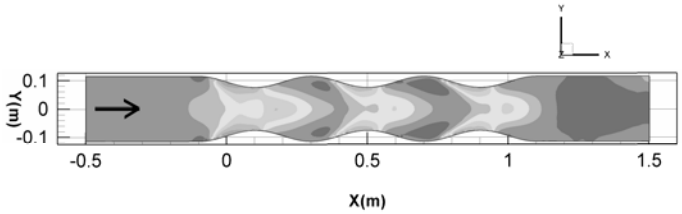

Figure 3. Plan view of computed bed changes in a channel with sinusoidal varying width.

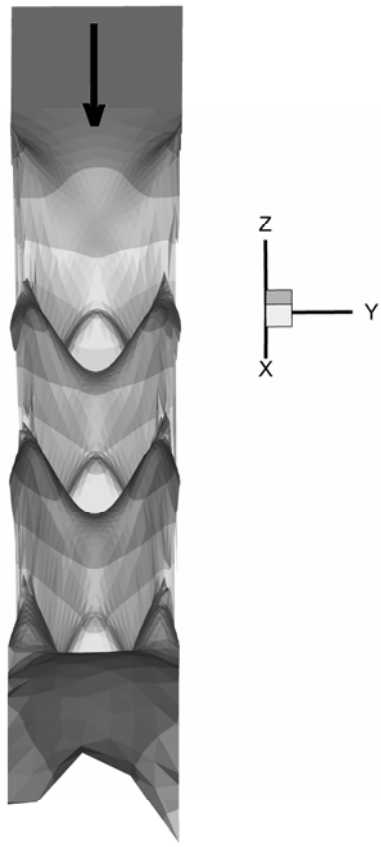

Figure 4. 3D view of computed bed changes in a channel with sinusoidal varying width.

4 DAM-BREAK OVER MOVABLE BED

Leal et al. (2002) performed dam-break experiments in a rectangular horizontal flume 19.2 m long, 0.5 m wide and 0.7 m high. The dam was simulated by a

vertical PVC lift-gate installed at the middle of the flume, which had an opening time between 0.1 and 0.2 s. The wave-front normally took less than 6 s to reach the downstream end of the flume. Three groups of tests were carried out depending on the bed type: fixed-bed, sand-bed and pumice-bed.

Two of the tests performed with an initial bed step of h_{su} = 0.19 m over a sand-bed were selected for the numerical simulation. The tests are Ts.25 and Ts.28, their initial conditions are shown in Figure 5 and Table 1. The initial conditions downstream from the dam varied between tests. The bed was dry for Ts.25 (h_d = 0.0 m) and wet for test Ts.28 (h_d = 0.075 m). The sand had a median grain size D_{50} = 1.22 mm, specific gravity G_s = 2.65 and settling velocity w = 9.92 cm/s.

Table 1. Initial conditions of experimental tests.

Test	h_u (m)	h_d (m)	h_{su} (m)	h_{sd} (m)
Ts.25	0.400	0.000	0.190	0.071
Ts.28	0.400	0.075	0.190	0.071

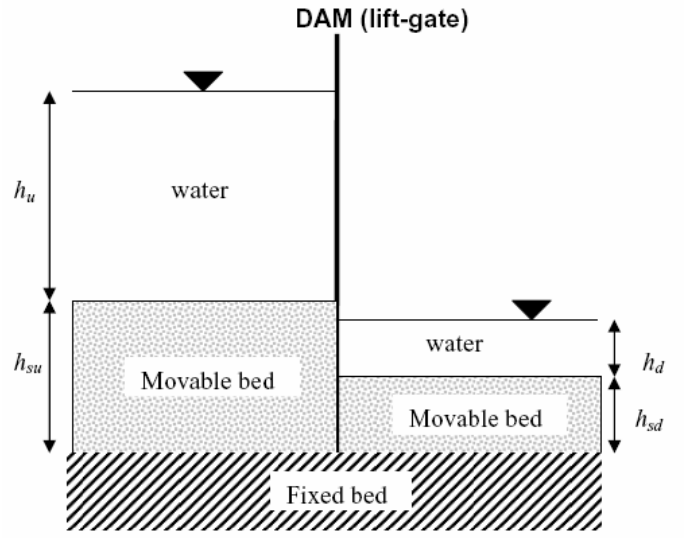

Figure 5. Initial conditions of Leal at al. (2002) experiments of dam-break over movable beds.

Leal et al. (2003a) applied the Bagnold sediment transport equation, which can be expressed as a function of the depth-averaged velocity $U = (u^2+v^2)^{1/2}$ as

$$q_s = \frac{\xi \tau_b U}{\rho g (G_s - 1)} \tag{15}$$

Where ξ is sediment parameter that depends on the sediment transport modes and settling velocity of the sediment and has a value $\xi \approx 0.57$ for the sand used in the experiments. Based on assumptions of sheet (debris) flow and bedload transport under high shear stress, Leal et al. (2003a) transformed (15) into

$$q_s = \frac{8.03\xi\sqrt{g}/C}{(G_s - 1)(C^2 - \xi U^2/h)} U^3 \tag{16}$$

With a value C = 31.3 m$^{1/2}$s for the sand-bed experiments.

5 RESULTS

Since the vertical bed step at the dam location cannot be reproduced in the model, it was replaced by a steep inclined ramp spanning over a single element. In order to reduce the size of the ramp, the node spacing in the mesh was set to about 5 cm. The computational mesh had roughly 12 nodes in the transverse direction and about 500 nodes in the longitudinal direction, as shown in Figure 6, giving a total of 6076 nodes and 10935 triangular elements. Figure 6 also shows the contour lines of the inclined ramp.

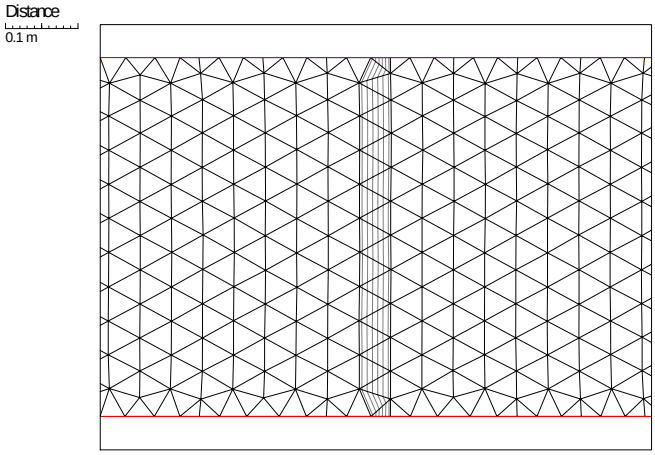

Figure 6. Detail of unstructured mesh near the dam location (dashed lines are bed contours of inclined ramp).

The roughness height adopted was k_s = 0.0164 m, which gives a Chezy roughness C = 31.3 m$^{1/2}$s for a water depth h = 0.075 m. The upstream boundary was set as a no-flow boundary; while the downstream boundary was set to a fixed water level, which changed according to the test simulated. For test Ts.25, the downstream water level was set equal to the bed elevation, h_{sd} = 0.071 m, meaning that all the reach downstream from the dam was initially dry, h_d = 0.0 m. For test Ts.28, the downstream water level was set at elevation $h_d + h_{sd}$ = 0.146 m. In both cases, the initial water level upstream from the dam was set to elevation $h_u + h_{su}$ = 0.590 m.

Similar to the initial bed profile, the initial horizontal water levels upstream and downstream from the dam were connected by an inclined water "ramp" over a single element, to represent the condition immediately after the dam break.

Figure 7 shows the results for test Ts.25, with an initially dry downstream boundary; while Figure 8

shows the results for test Ts.28, with an initial wet downstream boundary. The results for both tests are shown for 1 and 4 seconds after the dam-break. In both Figures are also presented the results of the two-layer 1D model of Leal et al. (2003a).

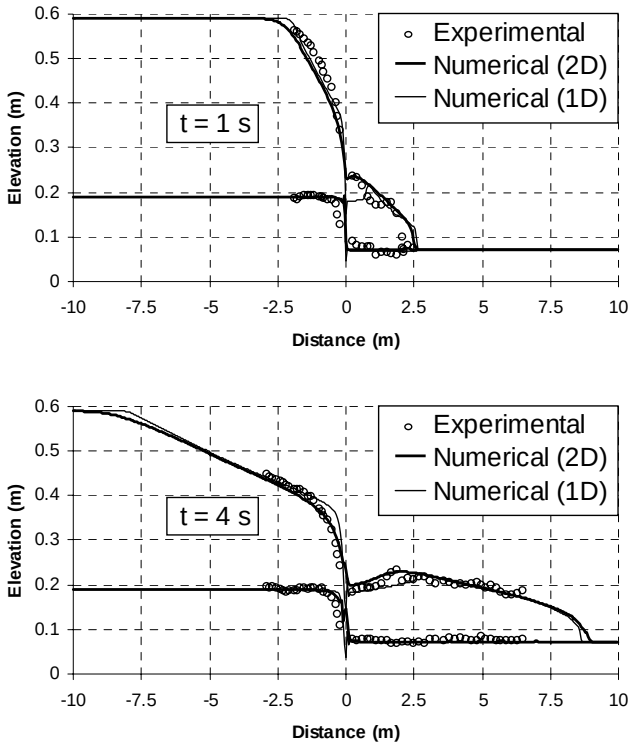

Figure 7. Experimental and numerical results for dam-break experiment Ts.25 at 1and 4 seconds.

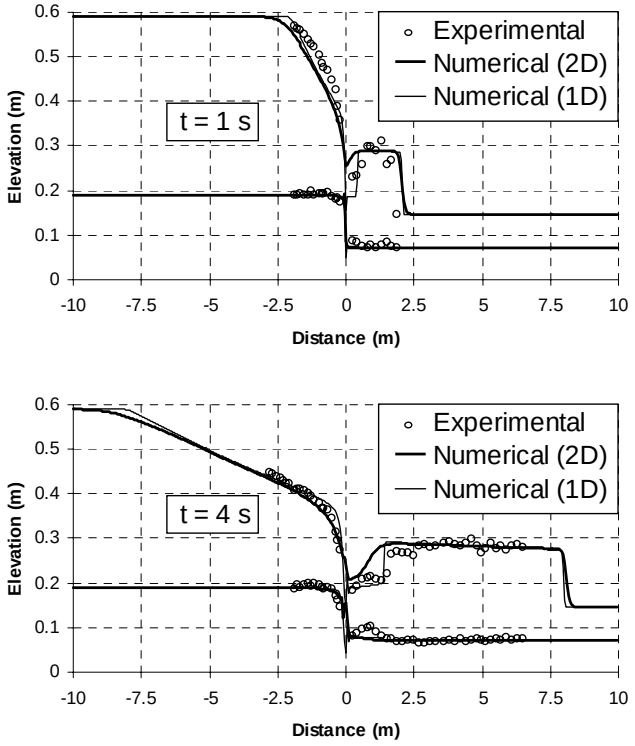

Figure 8. Experimental and numerical results for dam-break experiment Ts.28 at 1and 4 seconds.

By looking at the computed water levels upstream from the dam, for both tests the 2D model and the 1D model tend to underpredict the observed levels at 1 s. However, at 4 s, the agreement between the observed and computed water levels upstream from the dam is quite good.

For test Ts.25 (Fig. 7) both models underpredict the bed levels, while the agreement is better for test Ts.28 (Fig. 8). This is in accordance with what was expected, since for the higher initial downstream depth (Ts.28) the sediment transport is less important and the bed changes will be smaller.

6 DISCUSSION

In general, the agreement between measured and computed results is good. Just like the 1D model, the 2D model is able to capture the effects of the downstream water level on the wave fronts, with a weaker hydraulic jump when the bed is initially dry in test Ts.25. At 4 s, the upstream water levels agree very well with the observed data; although at 1 s the agreement is not as good. Probable reasons for the lower prediction accuracy at 1 s could be the assumed initial water profile (not perfectly vertical) and the non-hydrostatic pressure distribution. At the beginning of the experiment, immediately after the dam-break, the water contained upstream rushes down very quickly. The vertical acceleration of the flow is not negligible as assumed in the shallow water equations solved by the depth-averaged model. However, as time progresses, these initial effects tend to vanish (cf. Fraccarollo & Capart 2002) leading to a better agreement with data.

According to Fraccarollo & Capart (2002), the time required for the flow to equilibrate its sediment load is estimated as $20(h_u/g)^{0.5}$. For the experiments presented, this renders a time equal to 4 s. Therefore, for times equal or higher than that value the equilibrium approach assumed in both models is valid and the results show better agreement (t = 4 s in Figures 7 and 8).

The 1D model of Leal et al. (2003a,b), when applied to test Ts.25 and Ts.28 generated water surface profiles with very sharp fronts (wave-front and hydraulic jump), almost square in shape. In contrast, the profiles computed by River2D are smoother with more rounded corners. The 1D model uses a 2nd order MacCormack-TVD scheme that can reproduce better sharp discontinuities.

The discrepancies between the 1D and the 2D numerical results are more pronounced near the dam cross-section. In that section, at 1 s the 1D model imposes small water depths flow due to the initial bed-step, while the 2D model gives higher water depths. Nevertheless, the agreement is still good.

Mention should be made to the fact that the node spacing in both models is equal to 5 cm, therefore the resolution can not explain the differences mentioned before.

The computed bed elevation shows good agreement with the measured data, although some oscillations are visible in the solution, especially on the 1D model. The 2nd order 1D model creates oscillations around discontinuities. The TVD correction minimizes these oscillations. Due to mathematical complexity that correction was not applied to the sediment mass conservation equation, allowing the presence of oscillations in the bed profile. In the 2D model, the oscillations might be the result of applying the conventional Galerkin formulation to solve the sediment continuity equation, which is not suitable for highly convective problems (Donea & Huerta 2003, Katapodes 1984, Vasquez 2005a). Vasquez (2005a) has shown that when migrating bed forms are present in the solution (e.g. free alternate bars, prograding deltas), the bedload model produces spurious oscillations due to its lack of numerical upwinding. The Petrov-Galerkin scheme, which is used by the hydrodynamic model, seems as a good candidate for incorporating upwinding in future versions of the bedload model.

Although the 2D model solves a conventional sediment continuity equation with only one layer of sediment transport, the results are not significantly different to those obtained by the 1D model of Leal et al. (2003a) with a more complex two-layer model. It seems that for the present dam-break application, with relatively heavy bed material (G_s = 2.65), the effects of debris flow (sheet flow) are not strong enough to prevent the application of a 1-layer model. A comparative study between 1- and 2-layer models is desirable to gain a better understanding of the real limitations of each approach for dam-break analyses.

7 SUMMARY AND CONCLUSIONS

A 2D river morphology model, originally intended for alluvial meandering rivers, has been tested for dam-break flows over movable sand-beds. The model uses the Finite Element method and unstructured (irregular) meshes made of triangular elements. The model was tested using two experiments with an initial bed step at the dam location, with both dry and wet downstream boundary conditions. The model results were also compared with the results of the 1D model by Leal et al. (2003a). The results show that the 2D model was able to reproduce the observed water levels and the influence of the boundary condition on the wave fronts with reasonable accuracy. Given the other capabilities of the model to simulate bed changes in straight and curved alluvial channels, it seems as a promising tool for practical dam break analysis. However, the model still needs improvements to provide numerical upwinding in the sediment solver for cases of highly convective sediment waves.

REFERENCES

Aureli, F., Maranzoni, A. & Mignosa, P. 2004. Two dimensional modeling of rapidly varying flows by finite volume schemes. In Greco, Carravetta & Bella Morte (ed.) *River Flow 2004*: 837-847. London: Taylor & Francis Group.

Cao, Z., Pender, G., Wallis, S, & Carling, P. 2004. Computational Dam-break hydraulics over erodible sediment bed. *Journal of Hydraulic Engineering* 130(7): 689-703.

Capart H. & Young D.L. 1998. Formation of a jump by the dam-break wave over a granular bed. *Journal of Fluid Mechanics* 372: 165-187.

Donea, J. & Huerta, A. 2003. *Finite Element Methods for Flow Problems.* London: John Wiley & Sons.

Fraccarollo, L. & Capart, H. 2002. Riemann wave description of erosional dam-break flows. *Journal of Fluid Mechanics* 461: 183-228.

Ghanem, A., Steffler, P., Hicks, F. & Katapodis, C. 1995. *Two-dimensional modeling of flow in aquatic habitats.* Water Resources Eng. Report No. 95-S1. University of Alberta.

Heer, A. & Mosselman, E. 2004. Flow structure and bedload distribution at alluvial diversions. In Carravetta & Della Morte (eds) *River Flow 2004* (2): 801-806. London: Taylor & Francis Group.

Leal, J.G.A.B., Ferreira, R.M.L, Franco, A.B. & Cardoso, A.H. 2002. Dam-break waves on movable beds. In Bousmar & Zech (ed.) *River Flow 2002* (2): 981-990. Rotterdam: Balkema.

Leal, J.G.A.B., Ferreira, R.M.L. & Cardoso, A.H. 2003a. Dam-break waves propagation over a cohesionless erodible bed. *Proc. XXX IAHR Cong.,* Theme C(2): 261-268. Thessaloniki, Greece.

Leal, J.G.A.B., Ferreira, R.M.L., Cardoso, A.H. & Almeida, A.B. 2003b. Comparison between experiments and numerical results on dam-beak waves over dry mobile beds. Proceedings of the 3th IMPACT Workshop, Louvain-la-Neuve, Belgium, http://www.samui.co.uk/impact-project/cd3/de-fault.htm.

Leal, J.G.A.B., Ferreira, R.M.L. & Cardoso, A.H. 2006. Dam-break wave front celerity. *Journal of Hydraulic Engineering* 132(1): 69-76.

Katapodes, N.D. 1984. A dissipative Galerkin scheme for open channel flow. *Journal of Hydraulic Engineering* 110(4): 450-466.

Soares Frazão, S., Spinewine, B. & Zech, Y. 2001. Digital-imaging velocity measurements and numerical modeling of a dam-break flow through a 90° bend. *Proc. Of XXIX IAHR Congress, Beijing, 16-21 September 2001.* Beijing: Tsinghua University Press.

Soares Frazão, S. & Zech, Y. 2002. Dam-break in channels with 90° bend. *Journal of Hydraulic Engineering* 128(11):956-968.

Steffler, P.M. & Blackburn, J. 2002. *River2D:Two-dimensional depth averaged model of river hydrodynamics and fish habitat. Introduction to depth averaged modeling and user's manual.* Edmonton: University of Alberta.

Tsujimoto, T. 1987. Non-uniform bed load transport and equilibrium bed profile. *XXII IAHR Congress, Fluvial Hydraulics* (1): 177-182, Lausanne, Switzerland.

Vasquez, J.A. 2005a. Two-dimensional finite element river morphology model. PhD Thesis. University of British Columbia, Vancouver, Canada.

Vasquez, J.A. 2005b. Two-dimensional simulation of flow diversions. *17th Canadian Hydrotechnical Conference, Edmonton, 17-19 August 2005*.

Vasquez, J.A., Millar, R.G. & Steffler, P.M. 2005a. River2D Morphology, Part I: Straight Alluvial Channels. *17th Canadian Hydrotechnical Conference, Edmonton, 17-19 August 2005*.

Vasquez, J.A., Steffler, P.M. & Millar, R.G. 2005b. River2D Morphology, Part II: Curved Alluvial Channels. *17th Canadian Hydrotechnical Conference, Edmonton, 17-19 August 2005*.

Vasquez, J.A., Millar, R.G. & Steffler, P.M. 2005c. Two-dimensional morphological simulation in transcritical flow. In M. Garcia & G. Parker (eds) *4th IAHR Symposium on River, Coastal and Estuarine Morphodynamics*, *Urbana, 4-7 October 2005*. London: Taylor & Francis Group.

Vasquez, J.A., Millar, R.G & Steffler, P.M 2006a. Two-dimensional Finite Element River Morphology Model. *Canadian Journal of Civil Engineering*. Submitted.

Vasquez, J.A., Steffler, P.M & Millar, R.G 2006b. Two-dimensional Morphodynamic Model for Meandering Rivers based on Triangular Finite Elements. *Journal of Hydraulic Engineering*. Submitted.